

**MULTISCALE BEHAVIOR AND FRACTIONAL KINETICS FROM  
THE DATA OF SOLAR WIND - MAGNETOSPHERE COUPLING**

**G.M. Zaslavsky<sup>(1,2)</sup>, P. N. Guzdar<sup>(3)</sup>, M. Edelman<sup>(1)</sup>, M. I. Sitnov<sup>(3)</sup> and  
A. S. Sharma<sup>(4)</sup>**

<sup>(1)</sup>**Courant Institute of Mathematical Sciences, New York University,  
251 Mercer St., New York, New York 10012, USA**

<sup>(2)</sup>**Department of Physics, New York University, 2-4 Washington Place,  
New York, New York 10003, USA**

<sup>(3)</sup>**Institute for Research in Electronics and Applied Physics,  
University of Maryland, College Park, Maryland 20742, USA**

<sup>(4)</sup>**Department of Astronomy, University of Maryland,  
College Park, Maryland 20742, USA**

*09 November 2005*

*m-scale-pop.tex*

## ABSTRACT

Multiscale phenomena are ubiquitous in nature as well in laboratories. A broad range of interacting space and time scales determines the dynamics of many systems which are inherently multiscale. In most research disciplines multiscale phenomena are not only prominent, but also they have often played the dominant role. In the solar wind - magnetosphere interaction, multiscale features coexist along with the global or coherent features. Underlying these phenomena are the mathematical and theoretical approaches such as phase transitions, turbulence, self-organization, fractional kinetics, percolation, etc. The fractional kinetic equations provide a suitable mathematical framework for multiscale behavior. In the fractional kinetic equations the multiscale nature is described through fractional derivatives and the solutions of these equations yield non-convergent moments, showing strong multiscale behavior. Using a Lévy-flights approach, we analyze the data of the magnetosphere and the solar wind. Based on this analysis we propose a model of the multiscale features and compare it with the solutions of diffusion type equations. The equation with fractional spatial derivative shows strong multiscale behavior with divergent moments. On the other hand the equation with space dependent diffusion coefficients yield convergent moments, indicating Gaussian type solutions and absence of long tails typically associated with multiscale behavior.

## 1. INTRODUCTION

Many laboratory and natural systems have a broad range of interacting space and time scales and their dynamics exhibit multiscale features. The time-series data of such systems have some common characteristics: the physical variables reveal the properties often referred to as multiscale phenomena, heavy tails, strong intermittency, etc. Examples of such systems include dynamical systems with chaos, stock market indices, earthquakes, space and laboratory plasmas, atmospheric and hydrological systems, etc. A variety of characteristic quantities, such as Hurst exponents, multifractal spectra, Levy flights, etc. have been computed from the time series data using different approaches and techniques. Typically, the application of a specific method has been largely motivated by the current understanding of the relevant processes in a particular system, and their relationship to the available data.

From the dynamical systems point of view, the multiscale properties suggest fractal or multifractal structure of the dynamical processes and numerous simulations support this idea [1]. The advantage of the analysis of data generated by chaotic dynamics is a possibility to link the system evolution to the equations of the processes and to their origins, e. g., physical, chemical or biological processes. For example, the Lévy flights can be identified as dynamical processes of trapping into potential wells or ballistic propagation. Observing and analyzing different realizations of stochastic dynamical processes, one can classify them and apply the available techniques to the phenomena of which the details of the processes are not sufficiently known. A technique similar to the one used in the analysis of Lévy flights has been developed recently and has been applied to the plasma density fluctuations in the tokamak device [2]. Many studies of the solar wind - magnetosphere coupling have used the time series data to obtain the Hurst exponent characterizing the multiscale nature [3,4,5]. These studies have motivated the modeling of multiscale behavior in terms of well-known equations such as Fokker-Planck [6, 7] and Ginzburg-Landau equations [8].

It is however very desirable to apply different techniques to the same data set to obtain a consistent characterization of the underlying processes, and thus provide a strong basis for developing models. This point is underscored by the fact that the knowledge of the Hurst exponent [9, 10] does not provide sufficient information about the physical processes underlying the data. Indeed, the expression,  $\langle [x(t_1) - x(t_2)]^2 \rangle \sim |t_2 - t_1|^{2H}$ , which defines the Hurst exponent  $H$ , in fact, does not provide a clear and unique information about the random process  $x(t)$ . This is an important issue and three pertinent points are elaborated in the following.

First, the data typically characterize some specific physical observable  $x(t)$  and the Hurst exponent is strictly related to that observable. Other physical variables will have different exponents and the connection between these exponents is not known in the absence of more information about the real processes. Practically, it means that the common characterization as “subdiffusion” for  $H < 1/2$  and “superdiffusion” for  $H > 1/2$  have no real meaning unless the physical processes underlying the diffusion or, more generally, the kinetic processes, are specified. Second, the Hurst exponent is related to the second moment only, and does not reflect the behavior of other moments. For example, for Gaussian or Poissonian processes the second moment is sufficient to characterize the system as all higher moments can be expressed in terms of it. Some Gaussian type processes can have  $H < 1/2$ , and the higher moments can be evaluated from the data that yield the Hurst exponent. However, this feature can be revealed only by computing the higher moments. For the Lévy and other multiscale processes the second and higher moments are infinite. Such features are not captured by the Hurst exponent even if  $H > 1/2$  since, as mentioned above, the process may be superdiffusive, but it can not lead to a definite identification. Third, the Hurst exponent represents the time dependence of the variance but the time characteristic of the process, typically, is not sufficient, as is clear in the case of chaotic dynamics [1]. Indeed, the physical process can be characterized by a probability distribution function  $F(x, t)$  and the moments of  $x$  are defined as

$\langle x^m(t) \rangle = \int x^m(t) F(x(t), t) dx(t)$ . In order to distinguish, for example, a multiscale process from a Gaussian one, more subtle features from the data than just the Hurst exponent are needed. It should be noted that even for a purely diffusive process for which  $F(x, t)$  satisfies a kinetic equation with derivatives with respect to  $x$  and  $t$ , not only the exponent  $H$  is important for the kinetics but also the deviation  $\delta x$  during some specified interval  $\delta t$  is required.

The important role of kinetics was effectively demonstrated in [zaslavsky00, 2] where a new technique of data analysis was applied to the data of plasma density fluctuations in a tokamak. Assuming the presence of a Lévy-type multiscale process characterized by “flights”, a special procedure was used to separate the flight events without a characteristic scale from the “noisy” events with a characteristic small scale. The notion of “flight” is however non-trivial and it should be defined carefully to avoid ambiguity. It should be pointed out that recent studies of the data of space plasmas [6, 7] did not define the Lévy flights in their analysis. This issue deserves more careful attention [1]) and will be discussed in more detail in the following.

A simple way of introducing the notion of a Lévy-type flight, or in short, flight, is to consider a function  $x(t)$  or its integral(s) and obtain the long intervals  $\delta t$  where the changes in  $x(t)$  or its integral(s) are monotonic up to some level of accuracy. The change  $\delta x$  in  $x(t)$  is then a measure of the length of a flight with the distribution function  $F(\delta x, \delta t)$ , within the specified level of accuracy. It is very important to note that  $F(\delta x, \delta t)$  is the distribution of flights if they exist! Further, all moments  $\langle x^m(t) \rangle$ , obtained from the data, are always finite, i.e.,  $F(\delta x, \delta t)$  is truncated and defined up to  $\delta x_{max}$ ,  $\delta t_{max}$ . Then the extrapolation of  $F(\delta x, \delta t)$  should be carried out with utmost care. For example, in the case of  $F(\delta x, \delta t) \sim 1/(\delta x)^k$ , the moments  $\langle (\delta x)^q \rangle$  with  $q \geq k - 1$  will be infinite, but the observational data can yield the exponent  $k$  within the interval  $0 \leq \delta x \leq \delta x_{max}$ .

In this paper a specific form of Lévy flight analysis [2] to the data of the solar wind-magnetosphere coupling. A correlated dataset [11] of the magnetospheric dynamics

driven by the solar wind is used in this study. In this dataset corresponding to the last peak of the solar cycle, the solar wind (SW) is represented by the flow-induced electric field and the magnetospheric response is represented by the auroral electrojet index AL. This data set is used to study the multiscale properties by applying a technique based on an a priori assumption of the existence of Levy-like flights. This analysis yields a new characterization of the magnetospheric dynamics.

Multiscale behavior has been modeled using the so-called fractional generalization of the Fokker-Planck equation [1]. In order to determine the multiscale properties of such equations, numerical solutions of specific cases of such equations are studied. In the case of scale dependent diffusion coefficients it is found that the solutions of the equations yield convergent moments, and thus are not suitable for modeling the multiscale properties. In the case when the equations have fractional derivatives, viz. they represent fractional kinetics, and the numerical solutions do not yield convergent moments. It should be noted that the diffusion equation, even with a fractional time derivative representing the so-called fractal Brownian motion, has solutions in the form of a Gaussian function  $G(x/t^a)$ , for which all the moments are finite for any exponent  $a$ . In the case of a kinetic equation with a fractional derivative with respect to coordinate or momentum one can get the same exponent but only few (or even a single) first moments are finite, and all higher moments are infinite for any  $t$ . In the case when the kinetic process  $F(x, t)$  is modeled using the Fokker-Planck type equation with a scale dependent diffusion coefficients, as in [7], we show that all moments are finite. This leads to the conclusion that a correct exponent for the second moment alone is not sufficient to construct a model, and it is essential that the model yields the appropriate multiscale behavior.

The structure of the tails of the distributions of different physical observables becomes crucial (see also [12]), and as mentioned above, for data of finite length, defining the tail is a fairly sensitive task and needs confirmation from independent measurements. In particular, a specific demonstration is provided on how the accu-

racy of the data for the tail can be improved (see Fig. 4) if the relevant processes exhibit flights.

The structure of the paper is as follows. Section 2 presents a brief overview of the solar wind - magnetosphere interaction, the database and the recent studies relevant to this paper. In Sec. 3 the Lévy flight technique used to analyze the data [2] is described and also presents the corresponding results. The analysis indicate a power-law type behavior of the distribution functions in time and in the magnitudes of the fluctuations. The multiscale character of the observational data and some mathematical models for their description are discussed in Sec.4, followed by a detailed analysis of the fractional kinetic equation in Sec. 5. The reconstruction of the kinetic equations from the data is discussed in Sec. 6. Numerical studies of the fractional kinetic equation is described in Sec. 7, and the conclusions of the paper are summarized in Sec. 8.

## **2. COUPLED SOLAR WIND - MAGNETOSPHERE SYSTEM**

The Earth's magnetosphere is a huge cavity, mostly shielded from the flow of charged particles coming from the Sun, the solar wind plasma, by its magnetic field. The solar wind plasma can enter this magnetic shield through magnetic reconnection. The main source of plasma for the magnetosphere is the ionosphere, a relatively thin and dense plasma shell, which separates the magnetosphere from the Earth's thermosphere and atmosphere. The solar wind flow is not steady, because of the active solar corona, e. g., solar flares, coronal mass ejections and other bursty processes, as well as the inherent turbulent nature of the solar wind flow towards the Earth. Similarly, the magnetospheric activity is determined both by its interactions with the solar wind and by the complex internal activations on many scales occurring in the practically collisionless plasma of the magnetosphere. Attempts to classify the variety of observed phenomena have resulted in descriptive classifications such as magnetospheric storms, substorms, pseudo-breakups, convection bays, saw-tooth events, etc. Yet, the description remain essentially incomplete. Moreover, with some exceptions, e.g., the

storm-substorm relationship, they do not reflect important connections and similarities between processes occurring on different spatial and temporal scales, which are revealed both in the solar wind [13, 14] and in the magnetosphere [15, 16].

The recent studies of the multiscale behavior in the coupled solar wind - magnetosphere system have been based on two approaches. In the first, the observational data from different sources, such as spacecraft-borne and ground-based instruments, have been used to analyze the scaling properties. In the second approach, mathematical models such as Fokker-Planck type equations have been used to interpret these processes. In the latter equations which are known to exhibit multiscale properties are used to study the conditions under which the scaling laws and exponents derived from data can be obtained. However it should be noted that the ability of a particular type of equation to fit the data does not exclude other types of equations from reproducing the desired scaling, etc. Such studies provide valuable results that may lead to the origins of the multiscale behavior. These two approaches, viz. the studies using data and the modeling using equations, are discussed in the following sections.

The magnetospheric activity is characterized by a set of parameters, including both the basic physical ones, such as the magnetic and electric fields, plasma density etc., and the specific geophysical parameters or indices, e. g., Kp, Dst, AL, AU, AE, etc. [17]. A particularly relevant set of indices is the family of Auroral Electrojet indices AE, AU and AL, obtained from a number (usually greater than 10) of stations distributed in local time in the latitude region that is typical of the northern hemispheric auroral zone. For each of the stations the north-south magnetic perturbation H is recorded as a function of the universal time. A superposition of these data from all the stations yields a lower bound or maximum negative excursion of the horizontal component of the magnetic field variations, and is called the AL index. An upper bound, defined similarly, is called the AU index and the difference between these two indices, AU-AL, is called the AE index. Auroral indices are particularly relevant for substorm studies and have been used extensively for more general nonlinear time



series analysis and forecasting [18, 19] and for multiscale studies [16].

The scaling properties inherent in a data set can be represented by many characteristic parameters. One of the most popular is the Hurst exponent  $H$  [9, 10] measuring the "roughness" of multifractal data and allowing one to distinguish between conventional diffusion ( $H=0.5$ ), subdiffusion ( $H < 0.5$ ) and superdiffusion ( $H > 0.5$ ), as discussed earlier in Section 1. However, the presently available results for the Hurst exponent, computed largely from the AE index are rather controversial, can not distinguish between sub- and super-diffusion regimes. In particular, Takalo and Timmonen [3] found  $H=0.5$  based on the AE index studies. Uritsky and Pudovkin [20] concluded that  $H$  is largely less than 0.5 ( $H=0.38-0.59$ , depending on the sub-storm phase). In contrast, Price and Newmann [21] found that  $H$  is mostly greater than 0.5 ( $H=0.44-0.97$ , depending on the time scale range). In a series of studies involving extensive data processing, Hnat et al. [4, 5, 22] used different geophysical variables, including the solar wind parameter  $\epsilon$ , all three auroral indices, and the square of the interplanetary magnetic field  $B^2$ , to obtain the inherent scaling. These studies showed most of the Hurst exponents to be subdiffusive [7], with  $H$  ranging from 0.28 to 0.52. This is the most reliable result and it confirms the fractal nature of the solar wind. Overall, the observed data suggest subdiffusive behavior, which is drastically different from the superdiffusive behavior demonstrated by the widely used anomalous diffusion models utilizing the concept of Levy flights [1, 2, 23].

Attempts at resolving this ambiguity [24, 25] (see also [4, 5]) point out that only some of the parameters reveal the actual scaling corresponding to monofractals. A good example is  $B^2$  for the solar wind parameter [4]. In other cases either the generalized structure function (GSF) (depending on its order  $m$ ) or the probability distribution function (PDF), cannot be rescaled. Moreover, typically the effective  $H$ , inferred from the GSF of the order  $m=1$ , is more than 0.5, suggesting a superdiffusion, while  $H$  inferred for  $m > 1$  is equal to or less than 0.5, suggesting a subdiffusion. Another reason mentioned by Watkins et al. [25] is that almost any simulation of

fractional Levy motion is effectively one of truncated Levy motion, which may have the  $\zeta$  parameter of the GSF superdiffusive corresponding to the case for  $m=1$  and diffusive ( $H=0.5$ ) for  $m=2$ .

Thus, the GSF analysis shows that in many cases the solar wind and magnetospheric data do not show ideal scale invariance, that is, they do not correspond to a monofractal. And as a result, the simplest conclusions in terms of the Hurst exponents are too ambiguous and are not clear enough even to distinguish between sub- and superdiffusion behavior. On the other hand, Hnat et al. [5] revealed a collapse of the rescaled PDFs for the solar wind parameter  $\epsilon$  and the AE index, suggesting that some form of simple scale invariance may exist and may even allow one to distinguish between these scaling properties for the solar wind and the magnetosphere. According to Hnat et al. [22], this does not exclude the possibility that these scaling effects can be explained in terms of classical Fokker-Planck diffusion with scale-dependent diffusion coefficients. Finally, a fairly general analysis of the data [7] increases the level of ambiguity in the interpretation of the data.

The pitfalls of the data analysis in the case of multiscale processes, discussed in Section 1, leads to a couple of comments on the results from some recent studies [7, 8, 22]. First, in these papers the dispersion of the data in the tails is too high to draw a clear conclusion on whether a power-law tail exists. Second, the claim of a possible multifractality is not specified and, in fact, such behavior has two origins. One is that the data can have a few different scales (as it will be seen from our analysis in the following) in different intervals of  $t$ . This may not be a surprise since different physical processes may be responsible for different intervals of the magnetospheric data. The second source of multifractality is related to the so-called log-periodicity [1], i.e. a small modulation of the scaling law in  $\log t$  scale. This effect, while not discussed in [7, 8, 22], can be seen in Figs 1, 3, 4 of [7]. The existence of log-periodicity requires very different data analysis [1] in which the behavior of the higher moments becomes crucial.

The alternative approach to the data analysis and their interpretation, presented in the next section, is aimed at enhancing the information extracted from the observational data, and at improving the accuracy of its interpretation. It is worthwhile to add that this approach and technique have been developed building on the experience in the study of different models of dynamical chaos. The study of these models with the new technique has led to the improvements in its accuracy and has enabled one to verify some a priori assumptions on the character of processes with flights.

### 3. ANALYSIS USING LÉVY FLIGHT TECHNIQUE

Let  $y$  be a physical variable of interest, for example, the density of ions, or a component of the magnetic field, or the plasma current in a specified direction, and let  $y_i$  be its value at discrete time instant  $t_i$ . The time instants  $\{t_1, \dots, t_n\}$  are taken to be equidistant. It is also assumed that all data  $\{y_i\}$  are collected at the same location, i.e., the sequence  $\{y_i\}$  is a pure time-series at a specified point in space. Alternatively, the time series can represent the global behavior, e.g., the indices in the case of the magnetosphere.

The integrated value

$$S(t) = \int_0^t dy(t), \quad (1)$$

or, for a discrete time series  $\{t_i\}$ ,

$$S_n = S(t_n) = \sum_{j=1}^n y_j. \quad (2)$$

is used in the analysis of flights. In the case when the law of large numbers is valid, the fluctuations of  $S_n$  with respect to its mean value  $\langle S_n \rangle$  satisfy the condition

$$\langle |\delta S(t_N)|^2 \rangle = \langle |S_n - \langle S_n \rangle|^2 \rangle \sim N, \quad N \gg 1, \quad (3)$$

as in the case of Gaussian processes. In the anomalous case with power-law tails of the distribution of the values  $S_n$ , the relation (3) does not hold since the second or higher moments of the probability distribution function of  $\Delta S$ ,  $P(\Delta S)$ , are infinite

with

$$\Delta S_n \equiv S_n - n(y_n - y_0) \quad (4)$$

The corresponding processes are of Lévy type [26, 27]. The new variable  $\Delta S_n$  introduced in (4) differs from the integrated variable  $S_n$  by the subtraction of a linear trend. This replacement is done for convenience in working with the data, and it does not influence any physical interpretation of the results.

The solar wind induced electric field and auroral electrojet index [11] are used to compute  $\Delta S_{SW,n}$  and  $\Delta S_{AL,n}$  and the results are shown in Fig. 1. The results show large and small scale wiggles. A few zooms in Fig. 1(c,d) show a kind of self-similarity of the behavior of  $\Delta S_n$ , i.e., an indication of the presence of multiscales. Further analysis of the data can be done using a kind of pattern recognition scheme. Consider a set of connected values in Fig. 1 as a curve with many different segments and each segment is defined as an interval of a monotonic behavior of the curve  $\Delta S_n$ . Monotonicity of the curve  $\Delta S_n$  within an interval  $\Delta n_a = (n^{(1)}, n^{(2)})$  will be defined up to some interval  $a$  which is the interval of coarse-graining. This means that possible values of  $\Delta n_a$  form the set

$$\Delta n_a \in \{\Delta n_a\} = \{a, 2a, 3a, \dots\} \quad (5)$$

The monotonic piece of the curve  $\Delta S_n$  within an interval  $\Delta n_a$  will be called a “flight” and  $\Delta n_a$  is the duration of the flight. All flights are defined up to a smoothing interval  $a$ . The flights can be defined in both directions, i.e., as monotonic increases, or decreases of  $\Delta S_n$  within an interval of monotonicity.

The set of data of length  $\sim 10^5$  is used to compute the probability distribution function  $P_{SW}(n_a)$  and  $P_{AL}(n_a)$ , i.e. the distribution of the time duration of flights for the solar wind and auroral lower index, respectively. The corresponding results are shown in Fig. 2 for three different values of  $a = 2, 4$  and  $6$ . It is evident that the resulting curves do not differ strongly. The results for  $n_2$  ( $a = 2$ ) are chosen for detailed analysis, without a loss of generality.

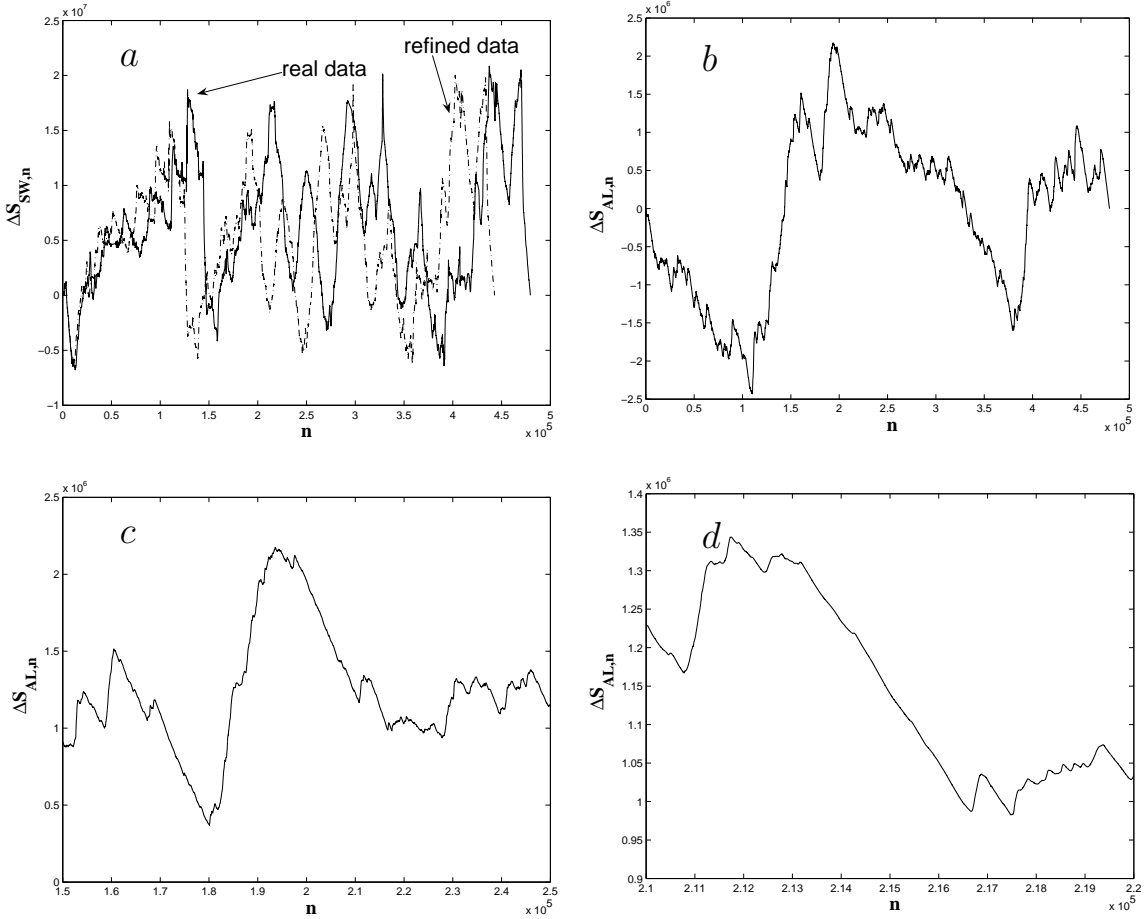


Figure 1: Coarse-grained data time series for the deviation  $\Delta S_{SW,n}$  (Solar Wind) and  $\Delta S_{AL,n}$  (Auroral Lower index) as a function of discrete time  $n$ : (a) real data (solid line) for  $\Delta S_{SW,n}$  and refined data with extrapolation of the data values for data gaps (dot-dashed line); (b) real data for  $\Delta S_{AL,n}$ ; (c) and (d) - zoom of the corresponding curves in (a) and (b).

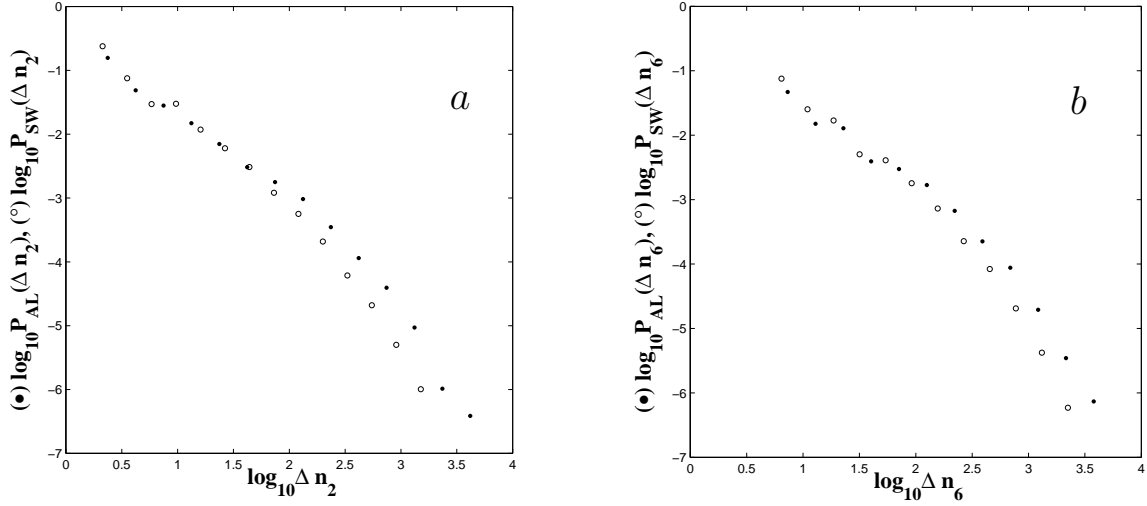


Figure 2: Plot of the distributions  $P(\Delta n)$  of the time-length  $\Delta n$  of “flights” for the solar wind (SW) and the magnetosphere (AL), with averaging over  $a = 2$  (a), and  $a = 6$  (b) points along  $n$ .

Both the distributions  $P_{\text{SW}}(n)$  and  $P_{\text{AL}}(n)$  have three characteristic segments defined by intervals of  $n$ : zone 1 (0 - 10), zone 2 (10 - 300), zone 3 ( $> 300$ ). In the first and third intervals the distributions can be written as

$$P(n) \sim \text{const}/n^{1+\beta} \quad (6)$$

where the exponent  $\beta_1$  depends on the type of data and on the interval. The computed values of the exponents are

$$\beta_{\text{AL}}^{(1)} \approx \beta_{\text{SW}}^{(1)} \approx 0.9 - 1.0$$

$$\beta_{\text{AL}}^{(3)} \approx 1.3 - 1.8$$

$$\beta_{\text{SW}}^{(3)} \approx 1.5 - 2.2 \quad (7)$$

The big error bar for zone 3 is due to an ill-defined width of the transition zone 2. The slope corresponding to AL appears to be smaller than that for SW in zone 3:

$$\beta_{\text{AL}}^{(3)} < \beta_{\text{SW}}^{(3)}, \quad (8)$$

and the accuracy of the computed values is higher, the larger is the value of  $a$  for the selected intervals of coarse-graining.

The transition zone 2 looks smoother for the solar wind data and one can assume that this zone corresponds to some *resonant type* process whose origin is in the solar wind. The response of the magnetosphere to the corresponding interval of flights duration makes the transition zone sharper.

Similarity of the behaviors of SW and AL data in zone 1 makes it possible to predict short flight evolution in the magnetosphere. A similar possibility to predict, though with a different probability, can be applied to zone 3.

There is a possibility to extract additional information from the data in Fig. 1. It is the change in the magnitude of  $S_n$  during a flight  $\Delta n_a$ . Let  $s$  be such a change and  $P_{SW}(s)$ ,  $P_{AL}(s)$  the probability distribution function for such changes. One can say that  $s$  is a change of the corresponding magnitude for an intermittent process during the period of monotonicity. Following the definitions (1), (2), and (4), during the monotonic flight between time instants  $t_1, t_2$  the value of  $s$  is

$$s_{12} = \text{const.}(t_2 - t_1) , \tag{9}$$

corresponding to the so-called *ballistic flights*, or

$$s_{12} = \text{const.}(t_2 - t_1)^2 \tag{10}$$

corresponding to the so-called *parabolic flights* with a constant acceleration. The corresponding distributions are given in Fig. 3 for two cases of coarse-graining:  $a = 2$  and  $a = 4$ , which do not show a difference. The results in Fig. 3 provide interesting observations. There are no 3 zones as in Fig. 2. The level of changes of  $s$  in SW is larger by almost an order of magnitude than in AL as it is seen from Fig. 1. The same difference is seen for the distribution functions from Fig. 3 within interval of  $s \in (10 - 300)$ . After  $s > 1000$  the PDF has the form

$$P(|s|) \sim \text{const}/|s|^{1+\alpha_1}, \tag{11}y$$

with  $\alpha_1$  given by

$$\begin{aligned}\alpha_{\text{SW}} &\approx 0.3 - 0.6, \\ \alpha_{\text{AL}} &\approx 0.7 - 1.\end{aligned}\tag{12}$$

The most interesting part of the distributions in Fig. 3 is that for  $s \gtrsim 1000$ , the difference between  $P_{\text{AL}}(|s|)$  and  $P_{\text{SW}}(|s|)$  is almost negligible for  $s \in (10^3 - 10^5)$ . This indicates that in this range of  $s$  the magnetosphere and the solar wind have similar characteristics. The studies of burst life time distributions [28] are closely related to these studies.

The above values of  $\alpha$  correspond to the super diffusive case. This is in contrast to the conclusion drawn from the values of the Hurst exponent, which has values  $< 0.5$  and thus corresponds to the subdiffusive case. As mentioned in the introduction, the explanation of the Hurst exponent needs more specific details of the physical processes and the corresponding theory (Secs. 4, 5; see also discussion in [4, 5, 25]). It should be noted that only some of the parameters reveal the actual scaling, corresponding to monofractals. A good example is the case of  $B^2$  in the solar wind [4]. In other cases either the generalized structure function (depending on its order  $m$ ) or the PDF cannot be rescaled, or both. Moreover, typically (say, for AE) the effective  $H$ , inferred from the  $m = 1$  GSF, is more than 0.5, suggesting a superdiffusion, while  $H$  inferred for  $m > 1$  is equal to or less than 0.5, suggesting a subdiffusion. It may be noted that a truncated Levy motion may also have the  $\zeta$  parameter of the GSF corresponding to superdiffusive for  $m=1$  and diffusive ( $H_{\text{effective}}=0.5$ ) for  $m = 2$ . The inconclusive nature of these studies was discussed in the previous section.

#### 4. MULTISCALE FEATURES IN OBSERVATIONAL DATA AND THEIR MATHEMATICAL MODELS

Many systems such as the coupled solar wind - magnetosphere system described in section 2 exhibit multiscale behavior in the form of power-law distribution of scale sizes or long tails in the probability distribution functions. The mathematical frame-



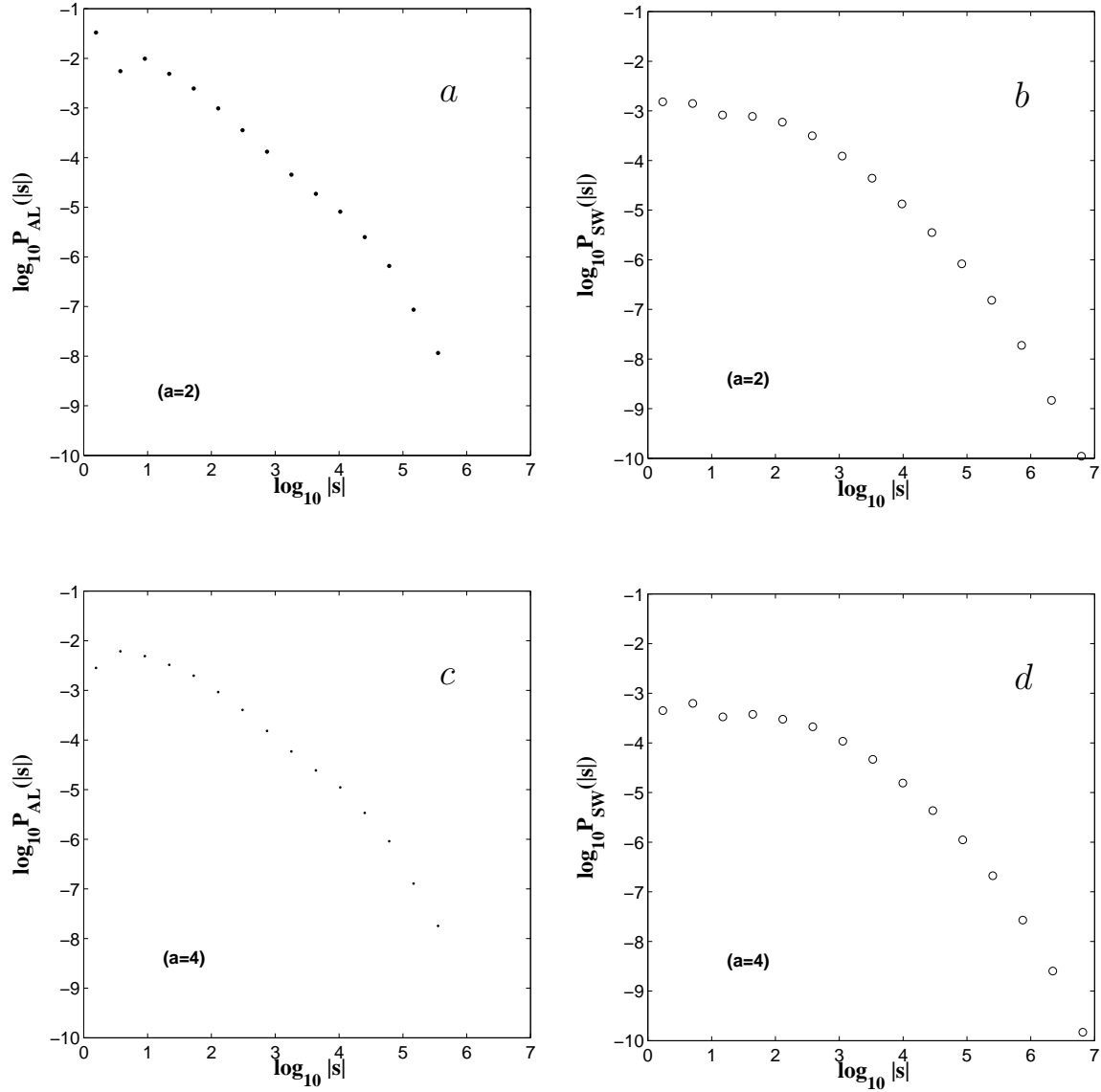


Figure 3: Plot of the distributions  $P(s)$  of the change  $s$  in the magnitude  $S_n$  per flight for the solar wind (SW) and the magnetosphere (AL).

work for modeling these phenomena, based on the diffusion-type equations, are described in this section.

For a system that exhibits self-similarity, the probability distribution function of a variable  $y(t)$  can be expressed as

$$F(y, t)dy = F(y/t^\nu)dy/t^\nu = F(\xi)d\xi, \quad (\xi = y/t^\nu). \quad (13)$$

The exponent  $\nu$  is to be determined from the dependence of the first moment on  $t$  as

$$\langle |y| \rangle = \int |y| F(y, t) dy = \text{const.} t^\nu, \quad (14)$$

with the symmetric  $F(y, t)$  and the normalization condition

$$\int F(y, t) dy = 1. \quad (15)$$

For example, if  $y$  is a coordinate that is subject to a diffusive type random walk process, then

$$\mu = 2\nu \quad (16)$$

and  $\mu$  is called the transport exponent since for the second moment

$$\langle y^2 \rangle = \text{const.} t^\mu. \quad (17)$$

The expression (17) needs further comments. The regular, or normal, diffusion has  $\mu = 1$ . Different values of  $\mu$ , including  $\mu = 1$ , can result from the Fokker-Planck type equation

$$\frac{\partial F(y, t)}{\partial t} = \frac{\partial}{\partial y} \mathcal{D}(y) \frac{\partial F(y, t)}{\partial y}, \quad (18)$$

depending on the function  $\mathcal{D}(y)$  that describes nonuniformity of the diffusion coefficient [29]. The main feature of the diffusion process is that  $F(\xi)$  decays exponentially as  $\xi \rightarrow \pm\infty$  and, as a result, all moments are finite:

$$\langle y^n \rangle < \infty, \quad 0 < t < \infty \quad (19)$$

for all  $n$ .

Another situation, when Eq. (19) is valid is the so-called case of sub-diffusion [30] described by

$$\frac{\partial^\beta F(y, t)}{\partial t^\beta} = \frac{\partial}{\partial y} \mathcal{D}(y) \frac{\partial F(y, t)}{\partial y} \quad (20)$$

where

$$0 < \beta < 1. \quad (21)$$

In Eq. (20) the time variation is described in terms of a fractional derivative of order  $\beta$ , and this is an example of a fractional kinetic equation. This and other forms of fractional kinetic equations will be discussed in more detail in the following. For  $\mathcal{D}(y) = \mathcal{D}_0 = \text{const.}$ , Eq. (20) gives

$$\langle y^2 \rangle = \text{const.} t^\beta, \quad (22)$$

which is slower than normal diffusion as a result of Eq. (21). In the both cases of Eqs. (18) and (20)  $F(y, t)$  have a characteristic width

$$\Delta \xi = \Delta y / t^\nu \quad (23)$$

such that for  $\xi \gg \Delta \xi$  the values of  $F(\xi)$  are exponentially small, which implies finite moments  $\langle y^n \rangle$  at any finite  $t$ .

The situation is very different when the probability distribution function  $F(y, t)$  behaves as

$$F(y, t) \sim \frac{c(t)}{y^{1+\delta}}, \quad \delta > 0, \quad t \rightarrow \infty, \quad y \rightarrow \infty, \quad (24)$$

where  $c(t)$  is a function of  $t$  alone. Then exponent  $\delta$  can be obtained as the slope in a  $\ln F(y, t)$  vs.  $\ln y$  plot. An important part of the data-derived models is a plot of a histogram of this dependence. The elementary connection between variations

$$\Delta \ln y = (1/|y|) \Delta y \quad (25)$$

for  $y \rightarrow \infty$  shows that a collection of the data of  $\ln F(y, t)$  into equal bins along the  $\ln y$  axis would provide less dispersion than the collection of the data into equal bins along the  $y$  axis. This statement is demonstrated in Fig. 4, where the log of the

probabilities  $P(\Delta n)$  for  $a = 2$  is plotted as a function of  $\ln \Delta n$  with bins of equal size in  $\Delta n$ .

Another, equally important comment is related to the truncation of  $F(y, t)$  for fairly large  $y$ , i.e., one should consider the data for  $F(y, t)$  and truncate part of the data for  $|y| > y_{\max}$  with  $y_{\max}$  that is not well defined. Let the experimental or simulation (called “raw”) data for a fixed  $t$  be within the interval  $y \in (y_0, y_1)$  and  $|y_1| \gg |y_0|$ . The power law distribution (24) imposes large fluctuations of the data for large  $|y|$  with a finite (though not exponentially small) probability. Independent of how big  $t$  is and how much larger  $y_1$  is compared to  $y$ , there will always be a lack of statistics close to  $y_1$ , and this is why some data within an interval  $(y_{\max}, |y_1|)$  has to be excluded.

There is a complementary result for the truncation of the raw data in all the moments

$$\langle |y|^m \rangle_{\text{tr}} < \infty, \quad (\forall m), \quad m > 0 \quad (26)$$

are finite and this permits the computation of the self-similarity and even the multi-fractality parameter  $\zeta(m)$  as

$$\langle |y|^m \rangle_{\text{tr}} \sim t^{\zeta(m)}, \quad (\forall m), \quad m > 0 \quad (27)$$

for the function  $F(y, t)$  if it exists. In the monofractal case

$$\zeta(m) = m\mu/2, \quad (28)$$

as compared to Eq. (17).

In reality, the multi-fractality can be due to the so-called log-periodicity [1], as discussed earlier. In particular, this means that there is some ambiguity in obtaining  $\zeta(m)$ ,  $\mu$ ,  $\delta$ , etc., which depend on  $y_{\max}$ . Thus for any exponent obtained from data, the interval for which it is computed and the quality of the statistics should be specified. Comparison of the exponents from different data sets must be within similar intervals of the definition of the exponents and for similar statistics.

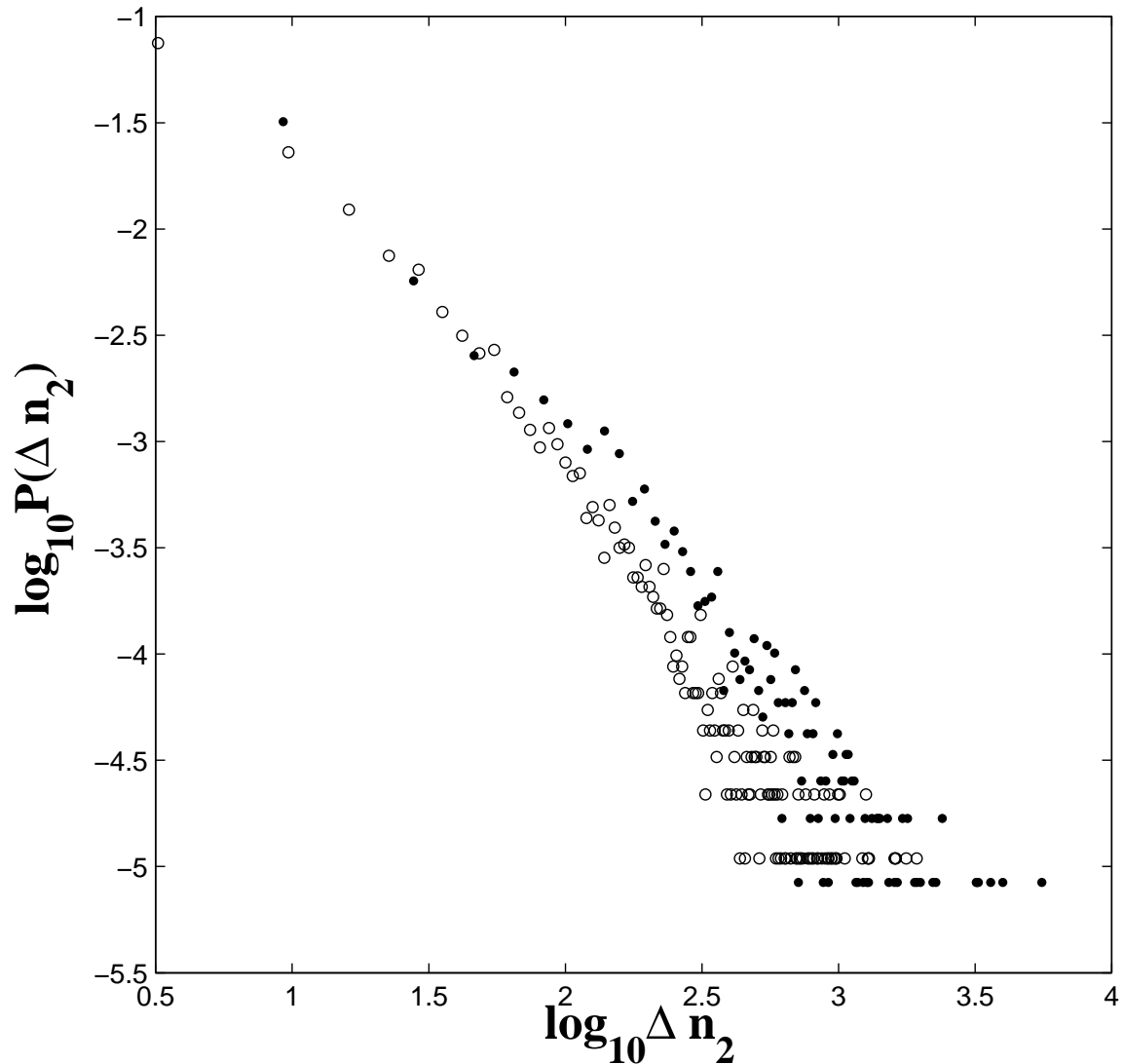


Figure 4: Log-Log plot of the distribution function  $P(\Delta n)$  with bins of equal sizes (equal to 2) in  $\Delta n$ , as compared to Fig. 2 where the bin sizes are equal in  $\log \Delta n$ . Dots are for the AL data and circles are for the SW refined data. The plot indicates a strong dispersion of the distribution, in comparison with the plot in Fig. 2.

## 5. FRACTIONAL PHENOMENOLOGY AND FRACTIONAL KINETICS

The crucial feature of the probability distribution function  $F(y, t)$  is the existence or non-existence of the stationary distribution  $F(y)$  for  $t \rightarrow \infty$ . In many physical problems there is no stationary distribution and the phase space of the problem has at least one unbounded variable. The plasma density fluctuations in laboratory fusion experiments (tokamaks) have been modeled in terms of a fractional kinetic equation [31]. Another example is the multiscale nature of the magnetosphere where the correlated data of the solar wind - magnetosphere system shows clear non-Gaussian PDF [32]. Zaslavsky [23] proposed a phenomenological approach to the nonstationary case of the evolution of  $F(y, t)$  in the presence of multiscale processes.

The basic approach is to write down a balance equation

$$\delta_t F(y, t) = \overline{\delta_y F(y, t)}, \quad (29)$$

where the bar implies averaging over all admissible paths. This equation can be written as

$$\delta_t F(y, t) = \Delta_t^\beta F(y, t) \quad (30)$$

where  $\Delta_t^\beta$  is a generalized difference operator for a time shift by  $\Delta t$  parameterized by  $\beta$  (see below). Similarly

$$\delta_y F(y, t) = \sum_{\Delta y} \Delta_y^\alpha [\mathcal{A}(\Delta y, y) F(y, t)] \quad (31)$$

where  $\Delta_y^\alpha$  is a generalized difference operator for a  $y$ -variable shift by  $\Delta y$  along a path  $\mathcal{A}(\Delta y, y)$  in the phase space, parameterized by  $\alpha$ , and the line in (29) implies averaging over all admissible paths. Definitions of  $\Delta_t^\beta$  and  $\Delta_y^\alpha$  are given in [1] and their main properties are

$$\begin{aligned} \Delta_t^\beta &\sim (\Delta t)^\beta \frac{\partial^\beta}{\partial t^\beta}, & (\Delta t \rightarrow 0) \\ \Delta_y^\alpha &\sim (|\Delta y|)^\alpha \frac{\partial^\alpha}{\partial |y|^\alpha}, & (|\Delta y| \rightarrow 0) \end{aligned} \quad (32)$$

where the fractional derivatives of the orders  $\beta$  and  $\alpha$ , respectively, are introduced. These derivatives work in different ways since there are different definitions of the variables  $t \in (0, \infty)$  and  $y \in (-\infty, \infty)$ .

To simplify the problem we consider  $F(y, t)$  to be symmetric with respect to  $y$  and  $\mathcal{A} = \mathcal{A}(\Delta y)$ . Then the balance equation can be written in the form [zaslavsky02, zaslavsky00; 1, 23]:

$$\frac{\partial^\beta F(y, t)}{\partial t^\beta} = \mathcal{D}_{\alpha\beta} \frac{\partial^\alpha F(y, t)}{\partial |y|^\alpha} \quad (33)$$

where

$$\mathcal{D}_{\alpha\beta} = \frac{|\Delta y|^\alpha}{(\Delta t)^\beta} \mathcal{A}(\Delta y), \quad \mathcal{A}(0) = \text{const.} \quad (34)$$

Eq. (33) is a fractional kinetic equation (FKE) [1, 23] since  $(\alpha, \beta)$  can be fractional. In the case of  $\beta = 1$ ,  $\alpha = 2$ , Eq. (33) is a regular diffusion equation with the diffusion coefficient  $\mathcal{D}_{\alpha\beta}$ . The important part of the derivation of (33) is the existence of finite  $\mathcal{D}_{\alpha\beta}$  in the limit

$$\Delta t \rightarrow 0, \quad \Delta y \rightarrow 0, \quad \mathcal{D}_{\alpha\beta} = \text{const.}, \quad (35)$$

known, for the case  $\beta = 1$ ,  $\alpha = 2$ , as the Kolmogorov condition [1]. The existence of the limit (35) is a nontrivial fact, and eventually it defines the variable  $y$  for which the FKE can be written.

An important property of Eq. (33) and the definition (34) is the rescaling invariance. Consider the following rescaling

$$\Delta y \rightarrow \lambda_y \Delta y, \quad \Delta t \rightarrow \lambda_t \Delta t \quad (36)$$

that gives

$$\mathcal{D}_{\alpha\beta} \rightarrow (\lambda_y^\alpha / \lambda_t^\beta) \mathcal{D}_{\alpha\beta}. \quad (37)$$

The FKE Eq. (33) is scale-invariant under the transforms (36) and (37) if

$$\beta / \alpha = \ln \lambda_y / \ln \lambda_t. \quad (38)$$

On the other hand, multiplying Eq. (33) by  $|y|^\alpha$  and integrating both sides over  $y$ , yields

$$\langle |y|^\alpha \rangle_{\text{tr}} = \text{const.} t^\beta, \quad (39)$$

i.e. the transport exponent

$$\mu = 2\beta/\alpha, \quad (40)$$

or using (38)

$$\mu = 2 \ln \lambda_y / \ln \lambda_t . \quad (41)$$

For  $\beta = 1$ ,  $0 < \alpha < 2$ , the FKE describes the Lévy process. The moments  $\langle |y|^p \rangle$  are finite if  $p < \alpha$  [30] and Eq. (39) can be considered only for the truncated  $F(y, t)$  as was commented on earlier.

In simple terms, if the data of a physical system exhibit the scaling property given by Eq. (36), then the FKE, Eq. (33), can be considered as a model of the processes the data represent.

## 6. FKE FROM THE DATA

The modeling of a physical system, whose data yields the scaling properties described in Sec. 2, in terms of a fractional kinetic equation is discussed in this section. There exists an indefiniteness in the reconstruction of the parameters  $(\alpha, \beta)$  that define the FKE. Starting with the rescaling parameters  $(\lambda_y, \lambda_t)$  obtained from data, only the ratio  $\beta/\alpha$ , but not the independent values of  $(\alpha, \beta)$  can be obtained. However, this indefiniteness does not influence the transport exponent  $\mu$ . Another indefiniteness of the data analysis arises from the Kolmogorov condition (35) since this information can not be obtained from the the time series data alone, and other approaches need to be employed.

In Sec. 2 the data of the solar wind - magnetosphere system were analyzed to obtain the distributions  $P(s)$  and  $p(t)$ . Since  $s$  is the accumulated variations in the variable, for example, the magnetic field in the solar wind during the time  $t$  of the duration of a flight, it is worthwhile to consider  $y = s/t$  as a measure of the physical variable within a flight. From the same data, one can obtain distributions presented in Fig. 5. By choosing

$$P(s/t) = P(y) = \frac{\text{const.}}{y^{1+\alpha_2}}, \quad (42)$$



where  $\alpha_2$  can be computed in the cases of the solar wind and the auroral electrojet index, and this yields

$$\alpha_{\text{SW}} \approx 2.0, \quad \alpha_{\text{AL}} \approx 2.1. \quad (43)$$

Then the results (7) and (43) give

$$\begin{aligned} \beta_{\text{SW}}^{(1)}/\alpha_{\text{SW}} &\approx \beta_{\text{AL}}^{(1)}/\alpha_{\text{AL}} \approx 0.45 - 0.5 \\ \beta_{\text{SW}}^{(3)}/\alpha_{\text{SW}} &\approx 0.75 - 1.1 \\ \beta_{\text{AL}}^{(3)}/\alpha_{\text{AL}} &\approx 0.62 - 0.86 \end{aligned} \quad (44)$$

The results (44) show that processes SW and AL are very close to each other in zone 1, related to small scale flights, and fairly different in zone 3 that is related to large scale flights.

In addition, for short flights the corresponding value of  $\mu$  is close to the normal one and even could be related to subdiffusion ( $\mu < 1$ ) while for the long flights  $\mu > 1$  and is related to superdiffusion processes if the variable  $y = s/t$  is the right one with respect to the Kolmogorov condition.

## 7. NUMERICAL STUDIES OF FRACTIONAL KINETIC EQUATIONS

In this section numerical results from the investigation of two classes of kinetic equations discussed earlier are presented. The first is the fractional kinetic equation (FKE) as defined earlier, Eq. (33), with  $\beta = 1$  and  $\alpha = 1.6$ . The second is the Fokker-Planck type equation, Eq. (18), but with a specific power-law dependence for the diffusion coefficient. For the sake of definiteness, the two equations are

$$\frac{\partial F(y, t)}{\partial t} = \frac{\partial^\alpha F(y, t)}{\partial |y|^\alpha} \quad (45)$$

$$\frac{\partial F(y, t)}{\partial t} = \frac{\partial}{\partial y} [ |y|^\mu \frac{\partial F(y, t)}{\partial y} ]. \quad (46)$$

For these studies  $\mu = 2 - \alpha$  to make the mean-squared displacement scale similarly with time for the two equations. For the FKE, a specific choice of the fractional

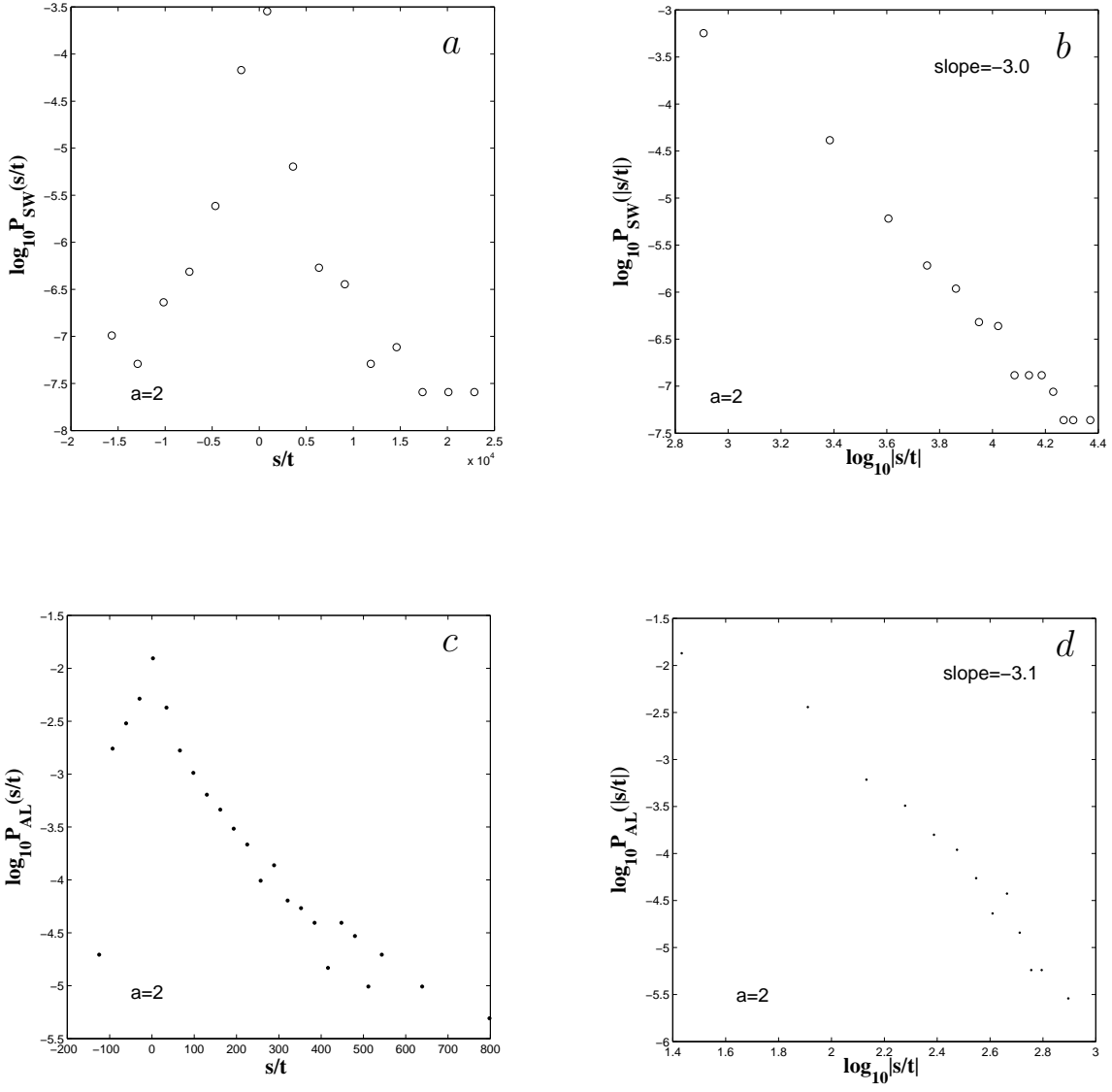


Figure 5: Distributions  $P(s/t)$  for SW (a) and AL (c) and their tails (b) and (d).

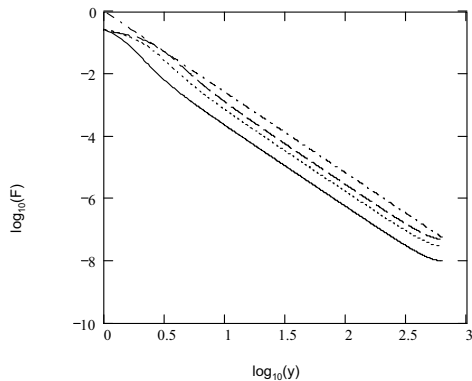


Figure 6:  $\log_{10}(F)$  versus  $\log_{10}(y)$  for  $t = 0.5$  (solid),  $t = 1.0$  (dot),  $t = 1.5$  (dash), asymptotic theory (dot-dash).

derivative in  $y$  has been made. For this choice, the Fourier transform representation for the dependent variable yields

$$\int_{-\infty}^{\infty} dy e^{iky} \frac{\partial^{\alpha} F(y, t)}{\partial |y|^{\alpha}} = -|k|^{\alpha} \hat{F}(k, t) \quad (47)$$

Here  $\hat{F}(k, t)$  is the Fourier transform of  $F(y, t)$ . Thus the solution in Fourier space of Eq. (45) is

$$\hat{F}(k, t) = \hat{F}(k, t_0) e^{-|k|^{\alpha}(t-t_0)} \quad (48)$$

For Eq. (46) an implicit finite difference scheme yields a tridiagonal equation which can be readily inverted to obtain the distribution function  $F(y, t)$  at different instants of time. Although the scheme is a stable one, the time-stepping restriction is determined by the requirement on accuracy.

Fig. 6 is a log-log plot for the solutions of Eq. (45) for  $\alpha=1.6$  at different instants of time. The different lines are for three instants of time namely,  $t = 0.5$  (solid),  $t = 1.0$  (dot),  $t = 1.5$  (dash). The last line (dot-dash) is the theoretically determined asymptotic solution derived in Sec. 4 (Eq. 40).

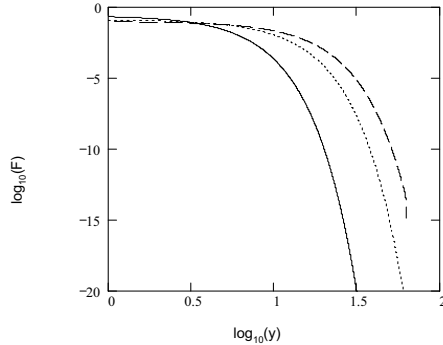


Figure 7:  $\log_{10}(F)$  versus  $\log_{10}(y)$  for  $t = 2.0$  (solid),  $t = 6.0$  (dot),  $t = 10.0$  (dash).

In Fig. 7 is shown the log-log plot of the solutions of Eq. 46 for  $\mu=0.4$  also at different instants of time. Once again the different lines are at  $t = 2$  (solid),  $t = 6$  (dot) and  $t = 10$  (dash). For this case the distribution does not display any power-law type behavior.

Furthermore in Fig. 8, the normalized even moments (to  $2n = 10$ ) are plotted for the Gaussian distribution (diamonds), Eq (46) (at  $t = 8$ ) (squares) and for the FKE at  $t = 1.5$  (circles). Here again it is clear that for Eq. (46) the moments are finite and comparable to the Gaussian case. However for the FKE the moments are large and dependent on the size of the computation box (i.e. maximum value of  $y$  used in the computation) and in principle are infinite as expected, based on the arguments presented in Sec. 4.

## 8. CONCLUSION

In the solar wind-magnetosphere interaction, multiscale features coexist along with the global or coherent features, and have been studied extensively using nonlinear dynamical techniques. The detailed properties of these phenomena are studied using

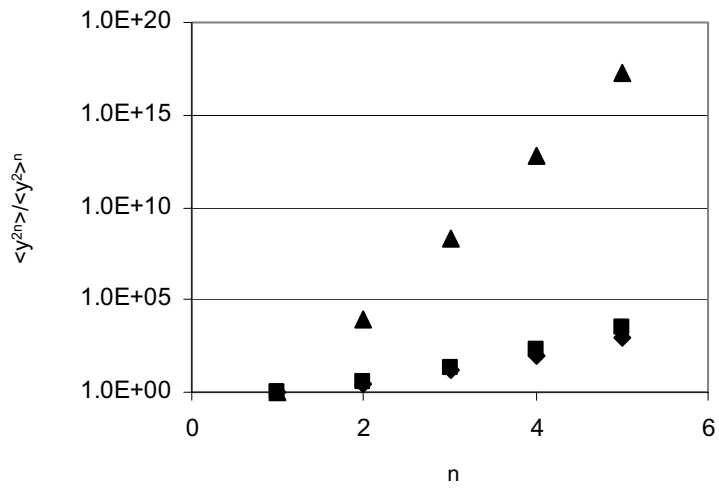


Figure 8:  $\langle y^{2n} \rangle / \langle y^2 \rangle^n$  versus  $n$  for Gaussian distribution function( diamonds), distribution function obtained from Fokker-Planck like equation (Eq. (46)) (squares) and distribution function obtained from the fractional kinetic equation (Eq. (45)) (triangles).

Levy flights and fractional kinetics models. In the solar wind - magnetosphere coupling, a technique to analyze the Levy-type processes is applied to the time series data of the solar wind electric field and the auroral electrojet index. The probability distribution function of the flights show similarities and differences, and provides a new insight into the origin of the multiscale behavior through the different values of the scaling indices. In a complementary approach, the fractional kinetic equations, which uses fractional derivatives to represent the complexity, provide a suitable mathematical framework for the multiscale behavior. Unlike the usual diffusion equations, the solutions of these equations yield non-convergent moments, showing its multiscale features. The origin of multiscale behavior is studied by using a fractional kinetic equation and a diffusion equation with a space dependent diffusion coefficient. Numerical solutions of these equations are used to analyze the nature of the equations by computing the moments. The fractional kinetic equations yield solutions with large moments and are divergent. On the other hand the solutions of the diffusion equation have convergent moments similar to those of Gaussian distributions. These results lead to the conclusion that the fractional kinetic equations are suitable models of multiscale phenomena.

In the the study of the solar wind by Hnat et al [5], all the probability distribution functions, e. g., their Figs. 3, 4, and 5, have infinite first moment because of the small Hurst exponent. However this does not follow from their equations (Eqs.(2) and (3)). This inconsistency raises the question of what leads to multiscale properties. In the studies presented in this paper, only the fractional kinetic equations lead to the formation of tails in the distribution functions, and thus can be considered as appropriate models of multiscale processes. It should however be noted that the parameters defining fractional kinetic equation could be improved as more data become available and with a better understanding of the magnetosphere dynamics.

## **ACKNOWLEDGMENTS.**

This work was supported by NSF / CMG grant DMS-0417800, and ONR grant N00014-02-1-0056. The simulations were supported by NERSC. The correlated data set of the solar wind - magnetosphere system used in this paper was compiled by Jian Chen.

## REFERENCES

- [1] G.M. Zaslavsky, Phys. Reports 371, 461 (2002)
- [2] G.M. Zaslavsky et al., Phys. Plasmas, 7, 3691 (2000).
- [3] J. Takalo and J. Timmonen, Geophys. Res. Lett., 21, 617, 1994.
- [4] B. Hnat et al., Geophys. Res. Lett., 29 (10), 10.1029/2001GL014587, 2002.
- [5] B. Hnat et al., Geophys. Res. Lett., 30, 2174, 2003.
- [6] S. C. Chapman et al., Submitted to Nonl. Proc. in Geophys., (2005).
- [7] N. W. Watkins et al., arXiv physics/0509058, v. 1, (2005).
- [8] L. Gil and D. Sornette, Phys. Rev. Lett., 76, 3991 (1996).
- [9] H. E. Hurst, Trans. Am. Soc. Civ. Eng., 116, 770 (2005).
- [10] J. Feder, "Fractals" (Plenum Press, New York, 1988).
- [11] J. Chen, A. S. Sharma, J. Geophys. Res., in press, 2005.
- [12] M. F. Shlesinger M.F. and M. A. Coplan, J. Stat. Phys. 52, 1423 (1988).
- [13] L. F. Burlaga, "Interplanetary Magnetohydrodynamics", (Oxford Univ. Press, 1995).
- [14] G. Consolini et al., Phys. Rev. Lett., 76, 4082 (1996).
- [15] B. T. Tsurutani et al., Geophys. Res. Lett., 17, 279 (1990).
- [16] G. Consolini, in "Cosmic Physics in the Year 2000", (1997).
- [17] P. N. Mayaud, "Derivation, Meaning, and Use of Geomagnetic Indices" (Amer. Geophys. Union, Washington, DC, 1980).
- [18] D. Vassiliadis et al., J. Geophys. Res., 100, 3495 (1995).
- [19] A. Y. Ukhorskiy et al., Geophys. Res. Lett., 31, L08802 (2004).
- [20] V. M. Uritsky and M. I. Pudovkin, Ann. Geophys., 16, 1580 (1998).

- [21] C. P. Price and D. E. Newmann, *J. Atm. Sol.Terr. Phys.*, 63, 1387 (2001).
- [22] B. Hnat et al., *Phys. Rev. E*, 67, 056404 (2003).
- [23] G.M. Zaslavsky, *Physica D*, 76, 110 (1994); *Chaos*, 4, 25 (1994).
- [24] N. W. Watkins et al., *Fractals*, 9, 471 (2001).
- [25] N. W. Watkins et al., *Space Sci. rev.*, in press (2005).
- [26] P. Lévy, “*Theorie de L’Addition Variables Aleatoires*” (Guthier-Villars, Paris, 1937).
- [27] V.V. Uchaikin and V.M. Zolotarev, “*Chance and Stability*”, (VCP, Utrecht, 1999).
- [28] M. P. Freeman et al., *Geophys. Res. Lett.*, 27, 1087 (2000).
- [29] H. Risken, “*The Fokker-Planck Equation: Methods of Solution and Applications*”, (Springer, Berlin, 1996).
- [30] A.I. Saichev and G.M. Zaslavsky, *Chaos* **7**, 753.
- [31] B. A. Carreras et al., *Phys. Plasmas*, 8, 5096 (2001).
- [32] A. Y. Ukhorskiy et al., *J. Geophys. Res.*, 107, 1369 (2002).